第40卷 第5期
2021年9月

岩 石 矿 物 学 杂 志
ACTA PETROLOGICA ET MINERALOGICA

Vol. 40, No. 5: 939~951
Sep., 2021

·综述与进展·

锆石微量元素地球化学对硅质火山岩浆系统的制约

贺振宇,颜丽丽
(中国地质科学院 地质研究所,北京 100037)

摘 要: 大型硅质火山作用(喷发体积约 $10^2 \sim 10^4\ km^3$)的岩浆系统是地壳尺度的,经历了复杂的起源、运移、存储、补给和喷发等过程。揭示岩浆从起源到喷发过程中的结晶分异、堆晶、晶体-熔体分离、地壳混染、岩浆补给、晶粥活化等岩浆作用的细节是认识硅质火山岩浆系统演化的关键。锆石中 Th、U、Ti、Hf 和 REE 等微量元素的含量和系统变化反映了锆石结晶熔体的成分、温度、氧逸度和水含量等以及共生的矿物相特征,对示踪火山岩浆系统的演化过程具有重要研究意义。随着岩浆温度降低过程中结晶分异作用的进行,锆石微量元素呈现出 Hf 含量升高、Ti 含量降低以及 Th/U、Eu/Eu* 和 Zr/Hf 等比值降低的趋势,这些元素含量和比值可以作为岩浆分异演化程度的指标。成矿斑岩中的锆石一般具有高的 Ce^{4+}/Ce^{3+} 和 Eu/Eu* 值,反映了岩浆具有高的氧逸度和水含量。火山岩锆石可能经历多阶段结晶过程,因而形成复杂的核-边结构特征,核部具有熔蚀现象,边部 CL 较亮并具有低的 Hf、U 和高的 Ti 含量以及 Eu/Eu* 值等,反映了岩浆补给作用和晶粥活化过程。由于锆石颗粒比较微小,在晶体-熔体分离过程可能随提取的熔体进入喷发岩浆房,从而可以连续记录岩浆成分的变化,或者残留在晶粥中记录晶体-熔体的分离。锆石微量元素结合高精度年代学分析,可以精细制约火山岩浆系统的多阶段演化过程及其时间尺度。在锆石微量元素数据的解释和筛选过程中,需注意扇形分区、锆石褪晶化和其他矿物包裹体对分析结果的影响,并同时开展岩相学研究,结合锆石产状和共生矿物组合特征,为制约火山岩浆系统的演化过程提供可靠信息。

关键词: 硅质岩浆系统;结晶分异;晶体-熔体分离;岩浆补给;锆石微量元素
中图分类号: P578.94+1;P588.11 **文献标识码:** A **文章编号:** 1000-6524(2021)05-0939-13

Zircon trace element geochemistry constrains on the silicic volcanic system

HE Zhen-yu and YAN Li-li
(Institute of Geology, Chinese Academy of Geological Sciences, Beijing 100037, China)

Abstract: The magmatic system of large silicic volcanic eruptions (with ejected volumes of about $10^2 \sim 10^4\ km^3$) extends through the crust, comprising complex generation, transport, storage, recharge and eruption processes. Critical aspect for understanding the evolution of silicic volcanic system is to reveal the magmatic processes from melt generation to eruption, such as crystal fractionation, crystal accumulation, crystal-melt segregation, crustal assimilation, magma recharge and mush rejuvenation. Zircon incorporates a variety of trace elements, such as Th, U, Ti, Hf and rare earth elements, and their abundances and variations are particularly sensitive to the composition, temperature, oxidation state, water content of the magma and the co-crystallized phases. Therefore, zircon has the outstanding capacity to record the evolution of silicic magmatic system. In general, as the falling temperature of the melt, the Hf concentration increases and the Ti concentration and Th/U, Eu/Eu* and Zr/Hf ratios typically decreases, which are effective indicators of fractionated magmas. Zircon from porphyry intrusions associated with

收稿日期: 2021-01-17;**接受日期:** 2021-06-11;**编辑:** 郝艳丽
基金项目: 国家自然科学基金(42002070, 42172070, 41772060)
作者简介: 贺振宇(1976-),男,博士,研究员,博士生导师,研究方向为火成岩岩石学,E-mail: ahhzy@163.com。
网络首发时间: 2021-06-16;**网络首发地址:** https://kns.cnki.net/kcms/detail/11.1966.P.20210616.1136.002.html

mineral deposits tends to have high Ce^{4+}/Ce^{3+} and Eu/Eu* ratios, indicating strong oxidized conditions and high water concentration. Zircon can show characteristics of multistage crystallization with a core-rim structure, including distinctly resorbed core and CL-bright rim. Compared to the zircon core, CL-bright rim commonly shows lower Hf and U and higher Ti and Eu/Eu* ratios, indicating magma recharge event and the rejuvenation of crystal mush. Due to the mobility of smaller zircon relative to the larger crystals, zircon may continuously be mobilized in extracting melts recording a continuous compositional range of magma evolution, but may also remain in the crystal mushes indicating crystal-melt segregation events. Zircon trace element compositions integrated by high-precision zircon U-Pb geochronology can track the evolution of silicic volcanic system as a function of time. Metamictization, sector zoning and exotic mineral inclusions should be considered to screen magmatic trace element signatures and interpret the zircon trace element data. Careful examination of thin sections of rock to find zircon occurring and associated minerals is also important to track the multiple evolution of silicic volcanic system.

Key words: silicic magmatic system; crystal fractionation; crystal-melt segregation; magma recharge; zircon trace element

Fund support: National Natural Science Foundation of China (42002070, 42172070, 41772060)

近年来的研究表明,大型硅质火山作用(喷发体积约 $10^2\sim10^4$ km^3)的岩浆系统是地壳尺度的,由深浅多个岩浆房相连构成,经历了复杂的起源、存储、运移、补给和喷发过程(图 1; Scandone *et al.*, 2007; Lipman and Bachmann, 2015; Bachmann and Huber, 2016; Cooper, 2017; Cashman *et al.*, 2017; Karakas *et al.*, 2019; 马昌前等, 2020)。目前关于硅质岩浆

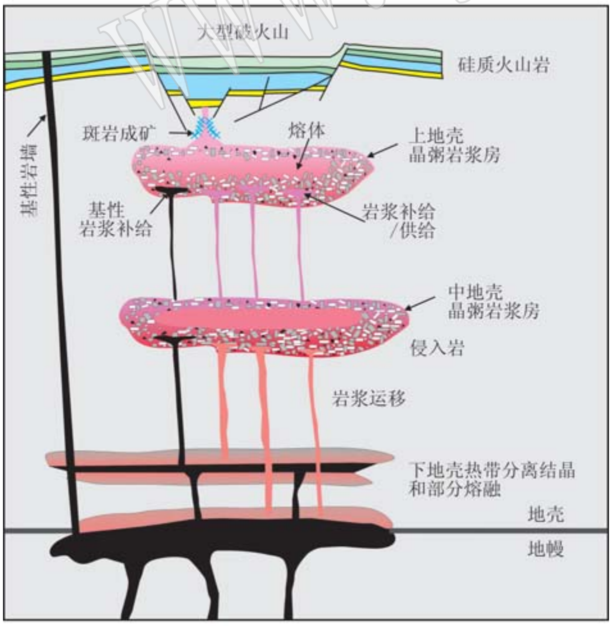

图 1 硅质火山作用的地壳尺度岩浆系统示意图[修改自 Yan 等(2016)、Bachmann 和 Huber(2016)]

Fig. 1 Schematic diagram of transcrustal silicic volcanic system (modified from Yan *et al.*, 2016; Bachmann and Huber, 2016)

的起源、岩浆在地壳岩浆储库的状态、火山喷发产物的成分与晶体含量不均一性的成因机制,以及火山岩与侵入岩的成因联系等问题,还存在许多不同认识,例如:幔源玄武质岩浆持续的分离结晶(或伴随有同化混染)被认为是硅质岩浆的主要形成方式(Annen *et al.*, 2006; Keller *et al.*, 2015; Frost *et al.*, 2016; Karakas *et al.*, 2017);幔源岩浆底侵导致下地壳岩石的部分熔融作用也可以形成硅质岩浆,但需要厚的成熟下地壳和能够阻挡幔源岩浆快速上升的密度和流变学条件(Dufek and Bergantz, 2005; Reubi and Blundy, 2009; Karakas *et al.*, 2017)。因此,分离结晶作用还是部分熔融作用对硅质岩浆起源起主导作用仍存在很大争议(Zimmerer and Mcintosh, 2012; Rooney and Deering, 2014; Keller *et al.*, 2015; Clemens and Stevens, 2016; 吴福元等, 2017)。另外,火山岩与侵入岩的成因联系也是一个长期争议的问题(Ustiyev, 1965; Lundstrom and Glazner, 2016),主要分歧在于侵入岩是否代表了火山岩浆提取之后的岩浆房中的残留体,还是仅仅是未喷出的火山岩岩浆(Bachmann *et al.*, 2007; Barth *et al.*, 2012; Zimmerer and Mcintosh, 2012; Gelman *et al.*, 2013; Glazner *et al.*, 2015; Lundstrom and Glazner, 2016)。

认识硅质火山岩浆系统的关键是揭示岩浆从起源到喷发过程中的结晶分异、堆晶、晶体-熔体分离、地壳混染、岩浆补给以及晶粥活化等岩浆作用过程的细节。地震成像、重力、电磁等地球物理研究手段能够重现火山岩浆管道系统的结构和演化以及熔体

的运移和岩浆房的组成状态等(Tibaldi, 2015; Pritchard *et al.*, 2018),例如地球物理成像研究揭示了中上地壳的岩浆房中熔体比例一般较低(低于20%),不支持岩浆房中物质以熔体为主的传统认识(Delph *et al.*, 2017; Magee *et al.*, 2018)。Dong 等(2020) 获得的深地震剖面揭示了我国东南沿海白垩纪火山-侵入杂岩带之下的中下地壳发育了大量的镁铁质岩席,可能提供了大规模硅质火山作用的地壳岩浆系统所必须的岩浆通量和热的地壳环境(Walker *et al.*, 2013; Bachmann and Huber, 2016)。岩石学和地球化学研究可以为制约硅质火山岩浆系统提供更加直接的信息,例如贫晶体火山岩及其包含的富晶体包体是岩浆房不均一和晶粥活化过程的直接证据(Burgisser and Bergantz, 2011; Huber *et al.*, 2012; Bachmann *et al.*, 2014; Foley *et al.*, 2020)。锆石($ZrSiO_4$)是硅质火山岩常见的副矿物,含有 Th、U、Ti、Hf、P 等多种微量元素和稀土元素,且具有较好的难熔性、稳定性,可保留其长期的结晶生长历史痕迹(Hoskin and Schaltegger, 2003)。近年来,随着高精度锆石 U-Pb 定年(CA-ID-TIMS,精度<0.1%, Schoene *et al.*, 2010)在精细制约火山岩浆系统的运移、存储、补给和成矿等过程的应用和发展,锆石微量元素地球化学也在相关研究中得到重视并发挥了巨大的作用(Mills and Coleman, 2013; Wotzlaw *et al.*, 2013; Samperton *et al.*, 2015; Deering *et al.*, 2016; Buret *et al.*, 2017; Szymanowski *et al.*, 2017; Ellis *et al.*, 2019)。本文着重介绍锆石微量元素地球化学在硅质火山岩浆作用过程方面的研究进展。

1　晶粥岩浆房与火山岩-侵入岩成因联系

关于硅质火山岩浆系统研究近年来的重要进展之一,是认识到岩浆房主要由晶粥组成,而不是以熔体为主,熔体比例高的可运移岩浆只占很小比例,呈透镜状位于岩浆房的顶部,且多个成分和物理性质不同的深浅岩浆房经由岩浆管道相连通,形成地壳尺度的岩浆系统(图 1; Caricchi and Blundy, 2015; Bachmann and Huber, 2016; Cashman *et al.*, 2017; Cooper, 2017; Xu *et al.*, 2020)。晶粥是一种晶体和熔体的混合物,由于具有高的晶体含量(50%~60%)和粘度,熔体的流动性和可喷发性有所降低,但晶体框架间的熔体会被抽取、汇聚,形成高硅火山岩浆,而残留的堆晶体和熔体固结形成侵入体(Bachmann and Bergantz, 2004; Hildreth, 2004; Miller and Wark, 2008; Cashman *et al.*, 2017)。晶粥模型较为合理地解释了硅质岩浆的成因、硅质火山岩的成分分层以及火山岩与侵入岩的成因联系等问题(Bachmann and Bergantz, 2004; Hildreth, 2004; 吴福元等, 2017; Bachmann and Huber, 2019; 马昌前等, 2020)。

由于硅质岩浆的粘度相对较大(达 10^5~10^6 Pas)且温度较低(一般<800℃),晶体-熔体的有效分离对于硅质岩浆尤其是高硅贫晶体岩浆的形成非常关键(Bachmann and Bergantz, 2004; 吴福元等, 2017; Bachmann and Huber, 2019),而熔体抽取之后富晶体残留的固结也是花岗岩体的重要形成方式之一(Miller and Miller, 2002; Weinberg, 2006; Lipman, 2007; 马昌前等, 2020)。当岩浆中晶体含量较低时(< 20%),主要通过晶体沉降方式实现晶体-熔体分离,但由于岩浆对流的影响,其效率很低;当晶体含量为 50%~70%时,可以通过压实方式有效实现晶体-熔体分离;而当晶体含量大于 70%时,晶体-熔体分离只有通过晶体变形压实作用才能实现,但这个过程尤其缓慢(Dufek and Bachmann, 2010; Holness, 2018; Bachmann and Bergantz, 2004; Bachmann and Huber, 2019)。此外,晶体-熔体分离的控制因素还有熔体的密度和粘度、晶体的密度、大小和形状以及岩浆中晶体-熔体-流体的比例等(Dingwell *et al.*, 1996; Scaillet *et al.*, 1998; Pistone *et al.*, 2017)。岩浆补给作用能够增加岩浆的温度和挥发分含量,引起晶粥的活化,促进晶体压实作用和晶体间熔体的运移(Parmigiani *et al.*, 2014; Pistone *et al.*, 2017; Bachmann and Huber, 2019)。

已有研究提供了晶粥岩浆房以及晶体-熔体分异演化的岩石学和地球化学证据,例如,在世界许多火山-侵入杂岩中普遍观察到了火山岩和侵入岩的成分间断,被认为是晶体-熔体分离作用的结果(Dufek and Bachmann, 2010; Sliwinski *et al.*, 2015; Deering *et al.*, 2016; Bachmann and Huber, 2016; Yan *et al.*, 2016, 2018a; 吴福元等, 2017);成分均一的大规模富晶体火山岩浆喷发,暗示了上地壳富晶体的岩浆房的存在以及岩浆补给-晶粥再活化过程(Bachmann *et al.*, 2002; Bachmann and Bergantz, 2003);贫晶体火山岩及其所含的富晶体包体,反映

了岩浆房成分分层及堆晶作用的信息(Burgisser and Bergantz, 2011; Huber *et al.*, 2012; Bachmann *et al.*, 2014; Foley *et al.*, 2020);不同阶段喷发产物的 SiO_2 含量、晶体含量、微量元素、温度、挥发分等差异形成的火山岩成分分层现象,记录了地壳岩浆系统的演化历史(Hildreth and Wilson, 2007; Bachmann and Huber, 2016)。因此,揭示岩浆的晶体-熔体演化过程和动力学对于理解硅质火山岩的成因以及破火山内高硅火山岩与低硅中央侵入体的成因关系具有重要意义。锆石能够连续地从岩浆中结晶,并可能随熔体迁移,或残留在晶粥中,因而锆石微量元素组成能够为反演硅质岩浆系统的演化过程提供重要信息。

2 锆石微量元素与岩浆的晶体-熔体演化

虽然锆石/熔体的分配系数在一定程度上受温度影响,但锆石微量元素含量及比值的系统变化主要反映了其结晶熔体的成分变化和共生矿物相,因而能够示踪岩浆的晶体-熔体演化过程(Luo and Ayers, 2009; Claiborne *et al.*, 2010; Reid *et al.*, 2011; Chelle-Michou *et al.*, 2014; Samperton *et al.*, 2015)。一般来说,随着岩浆分异演化,锆石微量元素呈现出 Hf 含量升高、Zr/Hf、Th/U 等比值降低的趋势,因此锆石 Hf 含量和 Zr/Hf、Th/U 等比值可以作为岩浆分异演化程度的指标(Claiborne *et al.*, 2006, 2010; Reid *et al.*, 2011; Wotzlaw *et al.*, 2013; Kirkland *et al.*, 2015; Samperton *et al.*, 2015)。斜长石优先容纳 Eu(图 2),其分离结晶可以导致熔体 Eu 亏损,结晶的锆石具有负的 Eu 异常($Eu/Eu^* < 1$),并随着岩浆分异程度增加,负异常增大(Trail *et al.*, 2012; Loader *et al.*, 2017)。锆石微量元素对熔体中富稀土元素矿物如榍石、磷灰石、角闪石等共生矿物也比较敏感。榍石、磷灰石、角闪石相对富集中稀土元素(图 2),它们从熔体中的分离结晶,能够"抵消"锆石 Eu 异常的程度,并产生中、重稀土元素比值(如 Sm/Yb、Dy/Yb 值)降低的趋势(Deering and Bacmann, 2010; Trail *et al.*, 2012; Wotzlaw *et al.*, 2013; Cooper *et al.*, 2014; Buret *et al.*, 2016; Loader *et al.*, 2017)。锆石 Ti 含量与温度呈正比,在 Ti 和 Si 活度已知的情况下,锆石 Ti 温度计可以用来估算锆石结晶时的熔体温度,进一步反演岩浆房的加热事件(如岩浆补给作用等)及岩浆的温度变化过程(图 3; Watson *et al.*, 2006; Ferry and Watson, 2007)。但需注意的是随着岩浆演化,Ti 和 Si 活度值可能发生变化,对温度估算结果会产生一定的影响,一般来说,估算温度与 Si 活度呈正比,而与 Ti 活度呈反比(图 3; Ferry and Watson, 2007; Claiborne *et al.*, 2010)。

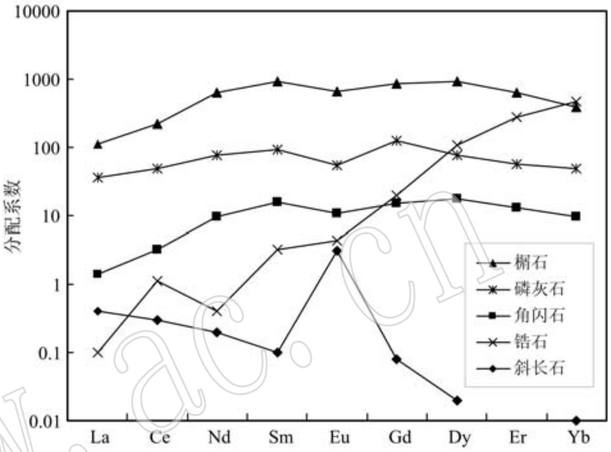

图 2 锆石、榍石、磷灰石、角闪石和斜长石的稀土元素分配系数(数据据 Sano *et al.*, 2002; Bachman *et al.*, 2005)

Fig. 2 Mineral-melt partition coefficients of REE for zircon, titanite, apatite, amphibole and plagioclase (data from Sano *et al.*, 2002; Bachman *et al.*, 2005)

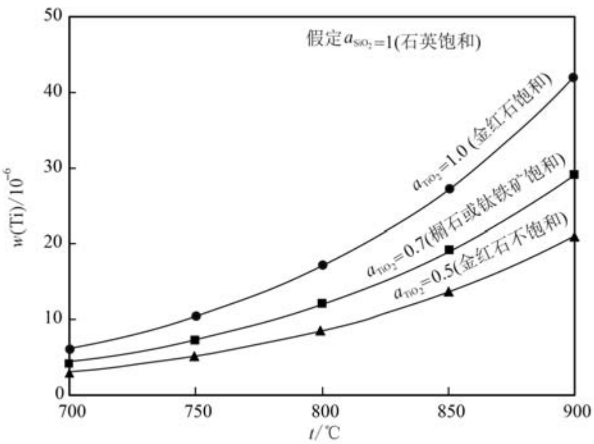

图 3 锆石 Ti 温度计估算结果[据 Ferry 和 Watson (2007)]

Fig. 3 Temperatures calculated by the Ti-in-zircon thermometer (Ferry and Watson, 2007)

对火山-侵入杂岩的锆石微量元素研究显示,火山岩与侵入岩的锆石微量元素含量变化范围大多具有重叠或部分重叠的特点,例如浙东雁荡山火山-侵入杂岩的流纹质熔结凝灰岩、流纹岩具有高的 SiO_2 含量(70%~76%),与破火山中央侵入相石英正长斑

岩的 SiO_2 含量（65%～66%）存在明显间断（Yan *et al.*, 2016；吴福元等，2017），但是它们的锆石微量元素含量却具有重叠的分布特点（图 4），而不具有类似主量元素的成分上间断，暗示了它们的锆石是在同一个岩浆房内连续结晶的，只是在晶体-熔体分离过程中随熔体发生了迁移，这为火山岩-侵入岩的成因联系提供了矿物学的证据。同时，这些锆石显示了微量元素方面的相关性，如 Hf 与 Ti、Y/Dy 与 Eu/Eu* 之间的负相关以及 Sm/Yb、Zr/Hf 与 Eu/Eu* 之间的正相关等（图 4），表明岩浆分异过程的分离结晶矿物主要有角闪石、榍石、磷灰石、斜长石、锆石等（Yan *et al.*, 2018b）。但是，火山岩与侵入岩的锆石微量元素组成有时也不具有重叠的变化范围，例如福建云山火山-侵入杂岩的高硅流纹岩和石英二长斑岩的锆石微量元素组成具有明显的区别。高硅流纹岩锆石具有高的 Hf、低的 Ti 含量和 Zr/Hf 值，而石英二长斑岩锆石具有低的 Hf、高的 Ti 含量和 Zr/Hf 值（图 5）。这一区别被解释为火山岩岩浆提取自含有早期结晶锆石的晶粥，但晶粥中锆石（及其它晶体）并没有随熔体迁移，晶体与熔体发生了分离，火山岩中低 Ti 含量和 Zr/Hf 值的锆石结晶自提取的火山岩岩浆，表明锆石微量元素也能够为示踪岩浆房的晶体-熔体分离过程提供重要线索（Yan *et al.*, 2020）。由于锆石在晶体-熔体分离过程可能随熔体迁移或残留在晶粥中，并可能在分异岩浆或补给岩浆中经历进一步的生长，因此在一些火山喷发产物中经常发育有复杂的锆石晶群（Barth *et al.*, 2012；罗照华等，2013；Stelten *et al.*, 2015；Deering *et al.*, 2016；Buret *et al.*, 2017；Zhang *et al.*, 2018）。

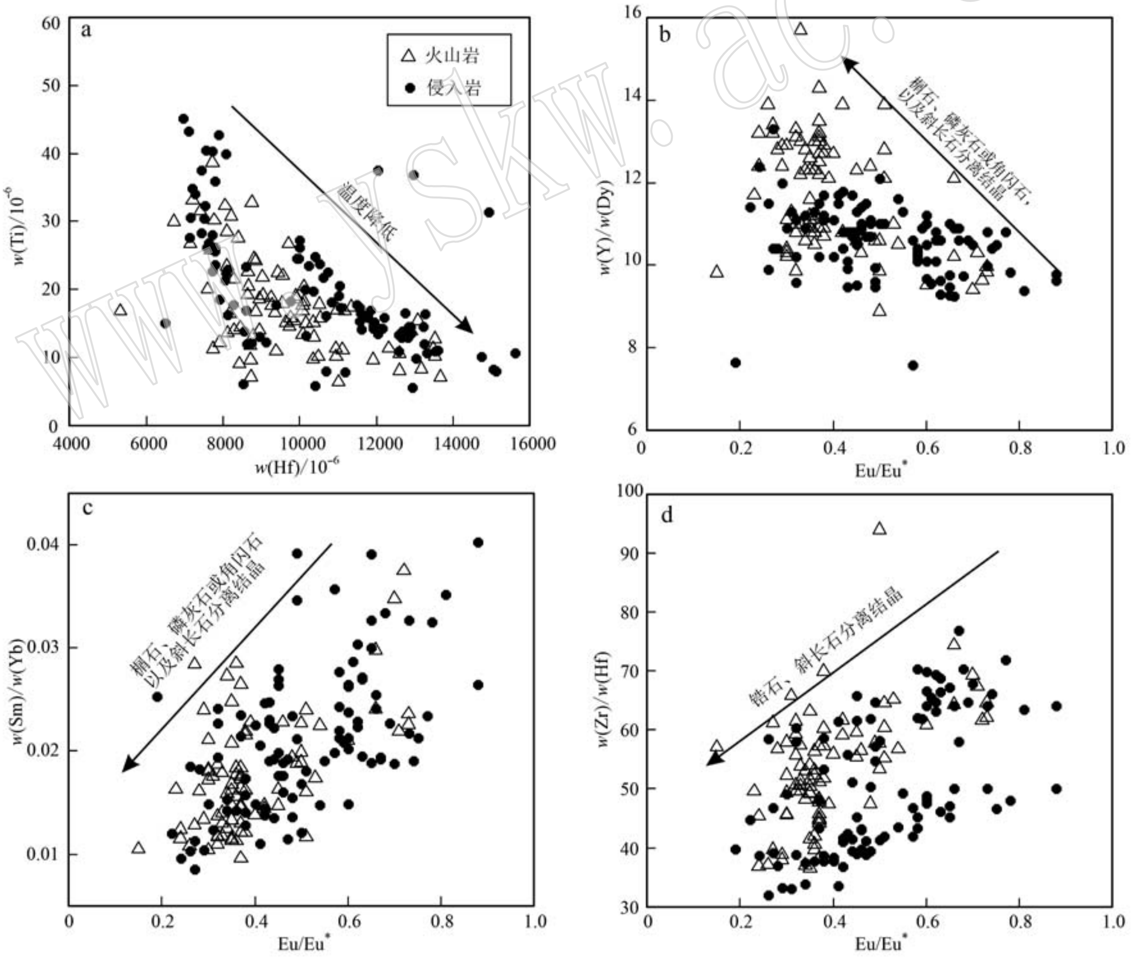

图 4　雁荡山火山-侵入杂岩的锆石微量元素组成（据 Yan *et al.*, 2018b）

Fig. 4　Trace element compositions in zircon from the Yandangshan volcanic-plutonic complex (data from Yan *et al.*, 2018b)

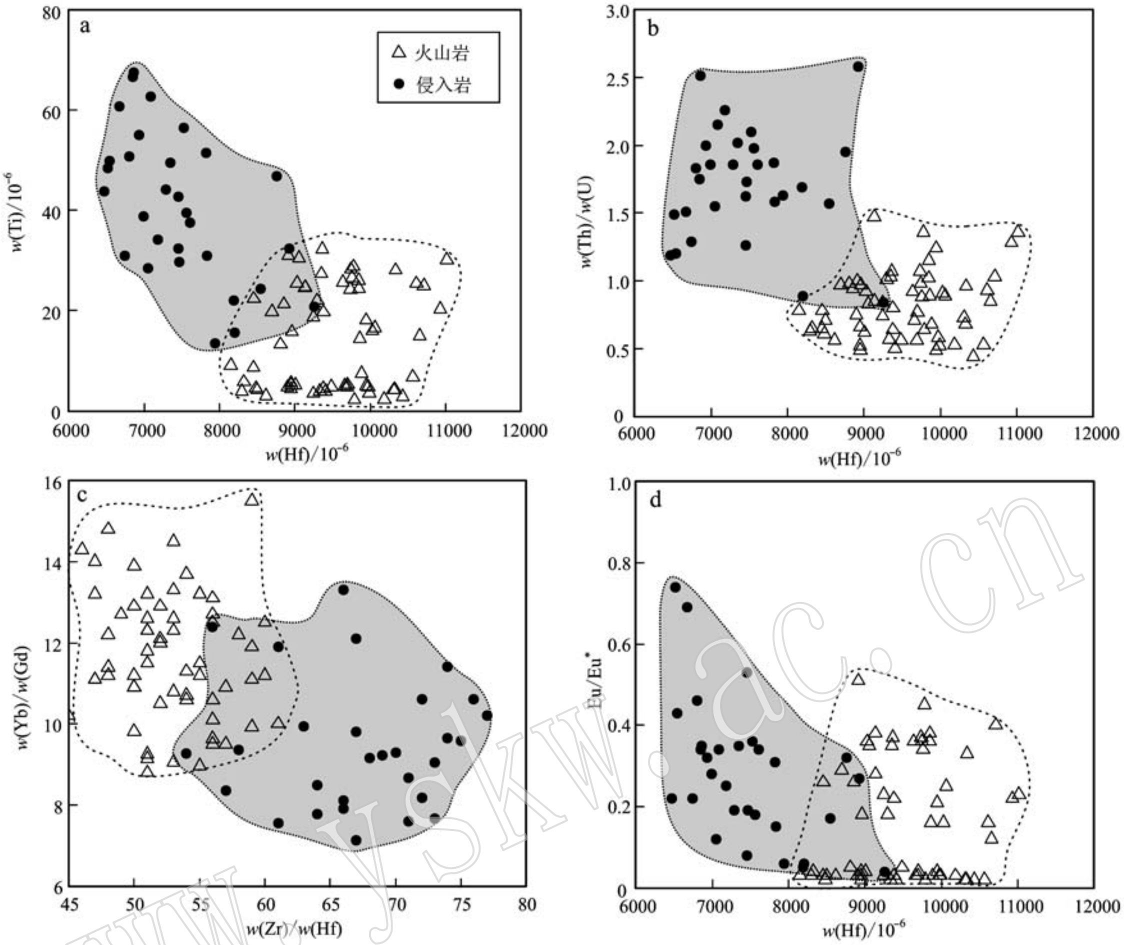

图5 云山火山-侵入杂岩的锆石微量元素组成(据 Yan *et al.*, 2020)

Fig. 5 Trace element compositions in zircon from the Yunshan volcanic-plutonic complex (data from Yan *et al.*, 2020)

3 锆石多阶段结晶与岩浆补给作用

岩浆补给作用一般是指热的、偏原始的岩浆周期性地注入较冷的、演化的岩浆房,反映了火山岩浆系统是开放的系统(Davidson and Tepley, 1997; Coombs *et al.*, 2003)。反复的岩浆补给作用能够增加岩浆房的压力和岩浆的挥发分含量,是触发火山喷发、导致喷发方式转变、引发成矿作用的重要因素(Pallister *et al.*, 1992; Murphy *et al.*, 2000; de Silva *et al.*, 2008; Kent *et al.*, 2010; Ruprecht and Bachmann, 2010; Buret *et al.*, 2016)。另外,岩浆补给作用为岩浆房补给热量和物质,促进岩浆对流、晶体-熔体的分离和堆晶体的重熔及再活化(Hildreth and Wilson, 2007; Lipman, 2007; Cooper, 2017; Pistone *et al.*, 2017; Bachmann and Huber, 2019; 马昌前等, 2020)。补给岩浆在一定条件下可以与原有岩浆一起喷发到地表,形成与火山岩成分不同的岩浆包体(Eichelberger *et al.*, 2000; Murphy *et al.*, 2000; Perugini *et al.*, 2007),但是在一些情况下,补给岩浆与原有岩浆来源相同或成分接近,补给作用往往表现的较为“隐蔽”(Eichelberger *et al.*, 2000; Bachmann and Huber, 2016)。岩浆冷却过程发生岩浆补给作用会导致岩浆成分及液相线温度的变化,产生锆石由饱和至不饱和的转变,增加 M 值[$M = (Na+K+2Ca)/(Al \times Si)$]和 Zr 含量及 Zr 饱和温度,导致已结晶锆石发生熔蚀和再结晶作用,形成具核-边结构等多阶段结晶特点的锆石,因此通过锆石微量元素组成研究可以反演岩浆补给作用和晶粥重熔作用过程(Claiborne *et al.*, 2010; Chamberlain *et al.*, 2014)。

美国科罗拉多州 San Juan 火山区的 Fish Canyon 凝灰岩以大规模喷发(>5 000 km^3)、具单一的英安质成分和富含晶体等特点,被视作晶粥活化喷发的

典型案例(Bachmann *et al.*, 2002; Bachmann and Bergantz, 2003)。研究者通过锆石微量元素分析结合质量平衡计算反演了 Fish Canyon 火山的岩浆中晶体含量的变化和晶粥活化的速率,结果表明在喷发前的 219 ka,岩浆中晶体含量高达 75%~80%,之后由于补给岩浆的底侵和扰动,晶粥发生重熔,晶体含量降低到喷发时的 45%,并触发了火山喷发(Wotzlaw *et al.*, 2013)。中国东南沿海火山-侵入杂岩的锆石也广泛发育核-边结构,具有多阶段结晶的特征,核部 CL 较暗、环带清晰,具有熔蚀结构,边部 CL 图像较亮、环带不明显(图 6)。CL 较亮的锆石,有时也可呈单独的颗粒(图 6b; He and Xu, 2012; Yan *et al.*, 2018b, 2020)。这类 CL 图像较亮的锆石一般具有低的 Hf、Yb、U 含量以及高的 Ti 含量和 Zr/Hf、Eu/Eu* 值,暗示了结晶自相对不演化的岩浆,并且锆石在高温、低演化岩浆中发生了熔蚀和再生长,反映了岩浆补给作用与晶粥活化过程(Chamberlain *et al.*, 2014; Yan *et al.*, 2018b, 2020)。应用锆石 Ti 温度计可以进一步制约原始岩浆与补给岩浆的温度变化过程。

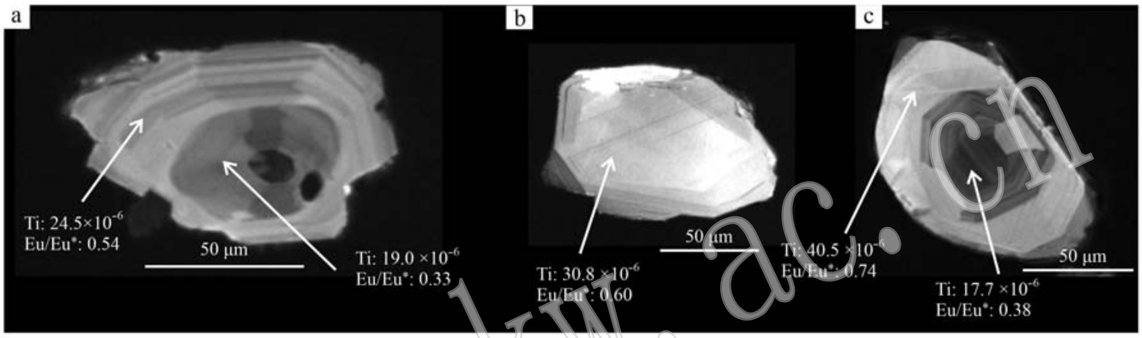

图 6　多阶段结晶锆石的阴极发光图像(据 Yan *et al.*, 2018b)

Fig. 6　Cathodoluminescence (CL) images of zircon formed by multistage crystallization (after Yan *et al.*, 2018b)

a、b—雁荡山流纹质火山岩; c—雁荡山石英正长斑岩

a and b—Yandangshan rhyolitic volcanic rocks; c—Yandagnshan porphyritic quartz syenite

4　锆石微量元素对斑岩成矿系统的制约

许多大型破火山根部的浅成斑岩体与 Cu、Mo、Au 等成矿作用具有密切的成因联系(Sillitoe, 2010)。岩浆补给作用引起火山岩浆复活在破火山内部形成浅成侵入体的同时(Lipman, 2007),对斑岩成矿系统的流体来源和演化也发挥了重要的作用,锆石微量元素能够示踪深部岩浆演化过程,从而揭示成矿过程的关键制约因素(Tapster *et al.*, 2016; Buret *et al.*, 2016, 2017; Zhang *et al.*, 2017)。例如,阿根廷 Farallón Negro 火山-侵入杂岩的 Bajo de la Alumbrera 斑岩铜矿的成矿作用与侵入相英安斑岩有关,Buret 等 (2016) 通过成矿斑岩的锆石中发育的暗色条带的微量元素组成揭示了岩浆演化过程中"隐藏"的岩浆补给作用。微量元素分析结果显示锆石中发育的 CL 暗色条带具有显著高的 Th、U 和稀土元素含量以及 Yb/Gd 和 Th/U 值,被认为与岩浆房冷却过程中高温基性岩浆补给事件有关:基性岩浆与冷的酸性岩浆接触发生淬冷,释放出富 CO_2 流体,导致酸性熔体中 H_2O 溶解度降低,引起锆石快速结晶,形成 CL 暗色的生长条带,之后由于 CO_2-H_2O 在酸性岩浆的进一步平衡,"正常"锆石继续生长。这一基性岩浆补给事件为斑岩成矿系统提供了必要的流体、硫和金属元素 (Buret *et al.*, 2016)。类似地,Large 等 (2018) 在新几内亚岛 Ok Tedi 的 Au-Cu 矿床的成矿斑岩中发现了两类锆石(高 Th/U 和低 Th/U),认为低 Th/U 类锆石来自安山质的补给岩浆,高演化岩浆的补给作用促进了岩浆-热液系统的演化和 Au-Cu 成矿作用。

成矿斑岩一般具有高的氧逸度与水含量,锆石的 Ce 和 Eu 异常程度能够反映岩浆氧逸度和水含量的变化。由于 Ce^{4+} 相对 Ce^{3+} 更易于进入锆石晶格,因此高的氧逸度会导致锆石 Ce 含量升高和 Ce^{4+} 相对 Ce^{3+} 富集,同时高的氧逸度和水含量会抑制斜长石的结晶,且 Eu^{3+} 不易进入斜长石,从而结晶锆石具有低的 Eu 异常程度(Ballard *et al.*, 2002; Trail *et al.*, 2012; Chelle-Michou *et al.*, 2014; Zhang *et al.*, 2017; Lee *et al.*, 2017; Loader *et al.*, 2017)。例如,智利 El Salvador 斑岩铜矿区成矿作用与斑岩密切相

关,早、晚两期形成的斑岩的锆石微量元素组成显示出两个不同的演化趋势:在低演化阶段(Hf 含量为 $9\ 000\times10^{-6}$),两期斑岩锆石均显示弱的 Eu 负异常(Eu/Eu* = 0.6~0.8),但随着岩浆演化(Hf 为 $12\ 000\times10^{-6}$ 时),早期贫矿斑岩锆石的 Eu/Eu* 逐渐降低到大约 0.4,而晚期富矿斑岩锆石仍显示高的 Eu/Eu* 值(0.6~0.7; Lee *et al.*, 2017)。

5 锆石微量元素数据与解释的影响因素

目前,研究者一般通过 LA-ICP-MS 或 SIMS (SHRIMP-RG)等分析方法获得锆石的微量元素含量(Claiborne *et al.*, 2010; Buret *et al.*, 2017; Coble *et al.*, 2018; Szymanowski *et al.*, 2018)。这些方法获得的锆石微量元素含量分析结果实际上是在分析束斑范围内(一般 20~50 μm)的混合结果,因此在数据解释过程中,需要注意不同环带、扇形分区以及锆石褪晶化、其它矿物包裹体等对分析结果的影响(Chamberlain *et al.*, 2014; Bell *et al.*, 2019; Zou *et al.*, 2019)。除了基于 CL 图像和透、反射光图像选择最合理的分析区域外,一些异常高的元素含量也能够指示分析数据的可靠程度,从而筛选出能够代表锆石真实微量元素组成的分析结果,如 Ca、Al、Na、K 指示长石和火山玻璃的影响,Ca、P、F 指示磷灰石的影响,Fe 指示 Fe-Ti 氧化物的影响,Ca 和 Fe 指示褐帘石的影响等。最近,Zou 等(2019) 提出了 La 指标,用 La ≤ 0.1×10^{-6} 来筛选"干净锆石",以简便可靠地识别矿物包裹体对分析结果的影响。Bell 等(2019) 提出 LREE-I 指标(LREE-I = Dy/Nd+Dy/Sm)来筛选受到后期蚀变或改造的锆石,LREE-I>50 的锆石被认为是未受蚀变或包裹体影响的岩浆锆石。

锆石常见的扇形分区也会导致微量元素分布的不均一,尤其体现在柱面(沿 *a* 轴和 *b* 轴生长)和锥面(沿 *c* 轴生长)微量元素含量上的区别,这种不均一性也是选取锆石微量元素分析点位以及使用微量元素分析结果反演火山岩浆演化时必须关注的问题(Reid *et al.*, 2011; Chamberlain *et al.*, 2014; Cooper *et al.*, 2014)。Chamberlain 等(2014) 揭示了美国加州 Long Valley 破火山 Bishop 凝灰岩中锆石颗粒的扇形分区特征,柱面 CL 较亮且 Ti、U、Th 含量较低,其(Sc+Y+REE^{3+})/P 值接近 1(反映磷钇矿替代机制),而锥面 CL 较暗且 Ti、U、Th 含量较高,其(Sc+Y+REE^{3+})/P 值相对较高(约 2.1~3),并且两类扇形分区的微量元素呈两个独立但平行的演化趋势。这种锆石微量元素组成差异与锆石生长速度较快导致的柱面和锥面微量元素未达到平衡有关(Watson and Liang, 1995; Watson, 1996),而不是反映了结晶自不同演化过程的熔体(Claiborne *et al.*, 2010; Chamberlain *et al.*, 2014; Cooper *et al.*, 2014)。

如前所述,火山岩浆会经历起源、存储、分异、补给和喷发等多个阶段的演化,在火山岩中可能会形成不同阶段结晶的锆石晶群,如自生晶(autocrysts)、前成晶(antecrysts)、残留晶(restites)、捕掳晶(xenocrysts)等(Miller *et al.*, 2007; Storm *et al.*, 2011; Pietranik *et al.*, 2013; Wotzlaw *et al.*, 2013; 罗照华等, 2013; Samperton *et al.*, 2015; Stelten *et al.*, 2015; Siégel *et al.*, 2018; Zhang *et al.*, 2018),因此,需要对这些不同来源的锆石晶群进一步区分,揭示它们的微量元素组成对于制约火山岩浆起源和演化过程的不同具体意义。锆石微量元素分析和高精度年代学相结合,能够为精确鉴别不同成因的锆石晶群提供信息,并揭示火山岩浆演化的时间过程。例如,美国黄石高原火山区是典型的硅质超级火山,经历了 3 期喷发事件(Watts *et al.*, 2012; Stelten *et al.*, 2015)。Stelten 等 (2015) 在破火山形成以后喷发的流纹岩的锆石中识别出边部的自生晶和核部的前成晶,认为前成晶随着从晶粥中提取的熔体运移进入喷发岩浆房,并且限定了这一过程的时间非常短暂(<6 ka),大量前成晶的存在还暗示了不同喷发期次火山岩浆之间的成因联系。但是,对于时代较老的火山活动产物(>100 Ma),即使采用高精度的年代学分析方法,分析误差也可能会超过岩浆作用过程的时间尺度。通过岩石薄片的锆石产状、结构、与其它矿物的包裹关系和原位微量元素组成的分析,结合基质和斑晶以及火山岩不同成分分层中锆石的晶型和微量元素组成对比,可以进一步限定锆石的生长演化历史以及锆石在晶体-熔体演化过程的行为,从而为通过锆石微量元素研究制约岩浆作用过程提供更加可靠的信息(Pietranik *et al.*, 2013; Słodczyk and Breitkreuz, 2014; Siégel *et al.*, 2018; Przybyło *et al.*, 2020)。

6 主要认识

锆石是硅质火山岩常见的副矿物,锆石微量元素如 Th、U、Ti、Hf 和稀土元素的含量和系统变化记

录了其结晶熔体的成分、温度、氧逸度和水含量及共生矿物等信息，在示踪火山岩浆系统的结晶分异、晶体-熔体分离、岩浆补给作用等演化过程以及揭示火山岩-侵入岩的成因联系、制约斑岩成矿系统的岩浆-热液系统演化等研究方面具有重要作用。锆石微量元素分析与高精度年代学研究相结合，可以精细揭示火山岩浆系统的多阶段演化过程及其时间尺度。在锆石微量元素数据的解释和筛选过程中，需注意不同扇形分区、锆石褪晶化和其他矿物包裹体对分析结果的影响，并结合锆石产状的岩相学研究，识别不同成因的锆石晶群，为制约火山岩浆系统的演化过程提供可靠信息。

致谢　评审专家对本文提出了十分有益的修改意见，在此表示诚挚的感谢。

References

Annen C, Blundy J D and Sparks R S J. 2006. The genesis of intermediate and silicic magmas in deep crustal hot zones[J]. Journal of Petrology, 47: 505~539.

Bachmann O and Bergantz G W. 2003. Rejuvenation of the Fish Canyon magma body: A window into the evolution of large-volume silicic magma systems[J]. Geology, 31(9): 789~792.

Bachmann O and Bergantz G W. 2004. On the origin of crystal-poor rhyolites: Extracted from batholithic crystal mushes[J]. Journal of Petrology, 45: 1 565~1 582.

Bachmann O, Deering C D, Lipman P W, *et al*. 2014. Building zoned ignimbrites by recycling silicic cumulates: Insight from the 1,000 km^3 Carpenter Ridge Tuff, CO[J]. Contributions to Mineralogy and Petrology, 167: 1~13.

Bachmann O, Dungan M A and Bussy F. 2005. Insights into shallow magmatic processes in large silicic magma bodies: The trace element record in the Fish Canyon magma body, Colorado[J]. Contributions to Mineralogy and Petrology, 149(3): 338~349.

Bachmann O, Dungan M A and Lipman P W. 2002. The Fish Canyon magma body, San Juan volcanic field, Colorado: Rejuvenation and eruption of an upper-crustal batholith[J]. Journal of Petrology, 43(8): 1 469~1 503.

Bachmann O and Huber C. 2016. Silicic magma reservoirs in the Earth's crust[J]. American Mineralogist, 101(11): 2 377~2 404.

Bachmann O and Huber C. 2019. The inner workings of crustal distillation columns; the physical mechanisms and rates controlling phase separation in silicic magma reservoirs[J]. Journal of Petrology, 60(1): 3~18.

Bachmann O, Miller C and de Silva S. 2007. The volcanic-plutonic connection as a stage for understanding crustal magmatism[J]. Journal of Volcanology and Geothermal Research, 167: 1~23.

Ballard J R, Palin M J and Campbell I H. 2002. Relative oxidation states of magmas inferred from Ce(Ⅳ)/Ce(Ⅲ) in zircon: Application to porphyry copper deposits of northern Chile[J]. Contributions to Mineralogy and Petrology, 144: 347~364.

Barth A P, Feilen A D G, Yager S L, *et al*. 2012. Petrogenetic connections between ash-flow tuffs and a granodioritic to granitic intrusive suite in the Sierra Nevada arc, California[J]. Geosphere, 8(2): 250~264.

Bell E A, Boehnke P, Barboni M, *et al*. 2019. Tracking chemical alteration in magmatic zircon using rare earth element abundances[J]. Chemical Geology, 510: 56~71.

Buret Y, von Quadt A, Heinrich C, *et al*. 2016. From a long-lived upper-crustal magma chamber to rapid porphyry copper emplacement: Reading the geochemistry of zircon crystals at Bajo de la Alumbrera (NW Argentina)[J]. Earth and Planetary Science Letters, 450: 120~131.

Buret Y, Wotzlaw J F, Roozen S, *et al*. 2017. Zircon petrochronological evidence for a plutonic-volcanic connection in porphyry copper deposits[J]. Geology, 45(7): 623~626.

Burgisser A and Bergantz G W. 2011. A rapid mechanism to remobilize and homogenize highly crystalline magma bodies[J]. Nature, 471: 212~215.

Caricchi L and Blundy J. 2015. The Temporal Evolution of Chemical and Physical Properties of Magmatic Systems[M]. London: Geological Society, Special Publications, 422: 1~15.

Cashman K V, Sparks R S J and Blundy J D. 2017. Vertically extensive and unstable magmatic systems: A unified view of igneous processes[J]. Science, 355: eaag3 055.

Chamberlain K J, Wilson C J, Wooden J L, *et al*. 2014. New perspectives on the Bishop Tuff from zircon textures, ages and trace elements[J]. Journal of Petrology, 55(2): 395~426.

Chelle-Michou C, Chiaradia M, Ovtcharova M, *et al*. 2014. Zircon petrochronology reveals the temporal link between porphyry systems and the magmatic evolution of their hidden plutonic roots (the Eocene Coroccohuayco deposit, Peru)[J]. Lithos, 198: 129~140.

Claiborne L L, Miller C F, Flanagan D M, *et al*. 2010. Zircon reveals protracted magma storage and recycling beneath Mount St. Helens

[J]. Geology, 38: 1 011~1 014.

Claiborne L L, Miller C F, Walker B A, *et al*. 2006. Tracking magmatic processes through Zr/Hf ratios in rocks and Hf and Ti zoning in zircons: An example from the Spirit Mountain batholith, Nevada[J]. Mineralogical Magazine, 70(5): 517~543.

Clemens J D and Stevens G. 2016. Melt segregation and magma interactions during crustal melting: Breaking out of the matrix[J]. Earth-Science Reviews, 160: 333~349.

Coble M A, Vazquez J A, Barth A P, *et al*. 2018. Trace element characterisation of MAD-559 zircon reference material for ion microprobe analysis[J]. Geostandards and Geoanalytical Research, 42: 481~497.

Coombs M L, Eichelberger J C and Rutherford M J. 2003. Experimental and textural constraints on mafic enclave formation in volcanic rocks [J]. Journal of Volcanology and Geothermal Research, 119: 125~144.

Cooper G F, Wilson C J, Charlier B L, *et al*. 2014. Temporal evolution and compositional signatures of two supervolcanic systems recorded in zircons from Mangakino volcanic centre, New Zealand[J]. Contributions to Mineralogy and Petrology, 167: 1 018.

Cooper K M. 2017. What does a magma reservoir look like? The "Crystal's-Eye" view[J]. Elements, 13: 23~28.

Davidson J P and Tepley F J. 1997. Recharge in volcanic systems: Evidence from isotope profiles of phenocrysts[J]. Science, 275: 826.

de Silva S, Salas G and Schubring S. 2008. Triggering explosive eruptions—The case for silicic magma recharge at Huaynaputina, southern Peru[J]. Geology, 36: 387~390.

Deering C D and Bachmann O. 2010. Trace element indicators of crystal accumulation in silicic igneous rocks[J]. Earth and Planetary Science Letters, 297: 324~331.

Deering C D, Keller B, Schoene B, *et al*. 2016. Zircon record of the plutonic-volcanic connection and protracted rhyolite melt evolution[J]. Geology, 44: 267~270.

Delph J R, Ward K M, Zandt G, *et al*. 2017. Imaging a magma plumbing system from MASH zone to magma reservoir[J]. Earth and Planetary Science Letters, 457: 313~324.

Dingwell D B, Romano C and Hess K U. 1996. The effect of water on the viscosity of a haplogranitic melt under PTX conditions relevant to silicic volcanism[J]. Contributions to Mineralogy and Petrology, 124(1): 19~28.

Dong S, Li J, Cawood P A, *et al*. 2020. Mantle influx compensates crustal thinning beneath the Cathaysia Block, South China: Evidence from SINOPROBE reflection profiling[J]. Earth and Planetary Science Letters, 544: 116 360.

Dufek J and Bachmann O. 2010. Quantum magmatism: Magmatic compositional gaps generated by melt-crystal dynamics[J]. Geology, 38(8): 687~690.

Dufek J and Bergantz G W. 2005. Lower crustal magma genesis and preservation: A stochastic framework for the evaluation of basalt-crust interaction[J]. Journal of Petrology, 46(11): 2 167~2 195.

Eichelberger J C, Chertkoff D G, Dreher S T, *et al*. 2000. Magmas in collision: Rethinking chemical zonation in silicic magmas[J]. Geology, 28: 603~606.

Ellis B S, Schmitz M D and Hill M. 2019. Reconstructing a Snake River Plain 'super-eruption' via compositional fingerprinting and high-precision U/Pb zircon geochronology[J]. Contributions to Mineralogy and Petrology, 174: 101.

Ferry J M and Watson E B. 2007. New thermodynamic models and revised calibrations for the Ti-in-zircon and Zr-in-rutile thermometers [J]. Contributions to Mineralogy and Petrology, 154: 429~437.

Frost C D, Frost B R and Beard J S. 2016. On silica-rich granitoids and their eruptive equivalents[J]. American Mineralogist, 101(6): 1 268~1 284.

Foley M L, Miller C F and Gualda G A R. 2020. Architecture of a super-sized magma chamber and remobilization of its basal cumulate (Peach Spring Tuff, USA)[J]. Journal of Petrology, 61(1): egaa020.

Gelman S E, Gutiérrez F J and Bachmann O. 2013. On the longevity of large upper crustal silicic magma reservoirs[J]. Geology, 41: 759~762.

Glazner A F, Coleman D S and Mills R D. 2015. The Volcanic-Plutonic Connection[M]. Berlin Heidelberg: Springer, 1~22.

He Z Y and Xu X S. 2012. Petrogenesis of the Late Yanshanian mantle-derived intrusions in southeastern China: Response to the geodynamics of paleo-Pacific plate subduction[J]. Chemical Geology, 328: 208~221.

Hildreth W. 2004. Volcanological perspectives on Long Valley, Mammoth Mountain, and Mono Craters: Several contiguous but discrete systems [J]. Journal of Volcanology and Geothermal Research, 136(3~4): 169~198.

Hildreth W and Wilson C J N. 2007. Compositional zoning of the Bishop tuff[J]. Journal of Petrology, 48: 951~999.

Holness M B. 2018. Melt segregation from silicic crystal mushes: A critical appraisal of possible mechanisms and their microstructural record [J]. Contributions to Mineralogy and Petrology, 173: 48.

Hoskin P W and Schaltegger U. 2003. The composition of zircon and igneous and metamorphic petrogenesis[J]. Reviews in Mineralogy and Geochemistry, 53: 27～62.

Huber C, Bachmann O and Dufek J. 2012. Crystal-poor versus crystal-rich ignimbrites: A competition between stirring and reactivation[J]. Geology, 40: 115～118.

Karakas O, Dufek J, Mangan M T, *et al*. 2017. Thermal and petrologic constraints on lower crustal melt accumulation under the Salton Sea Geothermal Field[J]. Earth and Planetary Science Letters, 467: 10～17.

Karakas O, Wotzlaw J F, Guillong M, *et al*. 2019. The pace of crustal-scale magma accretion and differentiation beneath silicic caldera volcanoes[J]. Geology, 47: 719～723.

Keller C B, Schoene B, Barboni M, *et al*. 2015. Volcanic-plutonic parity and the differentiation of the continental crust[J]. Nature, 523: 301.

Kent A J, Darr C, Koleszar A M, *et al*. 2010. Preferential eruption of andesitic magmas through recharge filtering[J]. Nature Geoscience, 3(9): 631～636.

Kirkland C L, Smithies R H, Taylor R J M, *et al*. 2015. Zircon Th/U ratios in magmatic environs[J]. Lithos, 212: 397～414.

Large S J, Quadt A V, Wotzlaw J F, *et al*. 2018. Magma evolution leading to porphyry Au-Cu mineralization at the Ok Tedi deposit, Papua New Guinea: Trace element geochemistry and high-precision geochronology of igneous zircon[J]. Economic Geology, 113(1): 39～61.

Lee R G, Dilles J H, Tosdal R M, *et al*. 2017. Magmatic evolution of granodiorite intrusions at the El Salvador porphyry copper deposit, Chile, based on trace element composition and U/Pb age of zircons [J]. Economic Geology, 112(2): 245～273.

Lipman P W. 2007. Incremental assembly and prolonged consolidation of Cordilleran magma chambers: Evidence from the Southern Rocky Mountain volcanic field[J]. Geosphere, 3: 42～70.

Lipman P W and Bachmann O. 2015. Ignimbrites to batholiths: Integrating perspectives from geological, geophysical, and geochronological data[J]. Geosphere, 11(3): 705～743.

Loader M A, Wilkinson J J and Armstrong R N. 2017. The effect of titanite crystallisation on Eu and Ce anomalies in zircon and its implications for the assessment of porphyry Cu deposit fertility[J]. Earth and Planetary Science Letters, 472: 107～119.

Lundstrom C C and Glazner A F. 2016. Silicic magmatism and the volcanic-plutonic connection[J]. Elements, 12: 91～96.

Luo Y and Ayers J C. 2009. Experimental measurements of zircon/melt trace-element partition coefficients[J]. Geochimica et Cosmochimica Acta, 73(12): 3 656～3 679.

Luo Zhaohua, Yang Zongfeng, Dai Geng, *et al*. 2013. Crystal populations of igneous rocks and their implications in genetic mineralogy [J]. Geology in China, 40(1): 176～181 (in Chinese with English abstract).

Ma Changqian, Zou Bowen, Gao Ke, *et al*. 2020. Crystal mush storage, incremental puton assembly and granitic petrogenesis[J]. Earth Science, 45(12): 4 332～4 351 (in Chinese with English abstract).

Magee C, Stevenson C T, Ebmeier S K, *et al*. 2018. Magma plumbing systems: A geophysical perspective[J]. Journal of Petrology, 59: 1 217～1 251.

Miller C F and Miller J S. 2002. Contrasting stratified plutons exposed in tilt blocks, Eldorado Mountains, Colorado River rift, Nevada, USA [J]. Lithos, 61: 209～224.

Miller C F and Wark D A. 2008. Supervolcanoes and their explosive supereruptions[J]. Elements, 4: 11～15.

Miller J S, Matzel J E, Miller C F, *et al*. 2007. Zircon growth and recycling during the assembly of large, composite arc plutons[J]. Journal of Volcanology and Geothermal Research, 167(1～4): 282～299.

Mills R D and Coleman D S. 2013. Temporal and chemical connections between plutons and ignimbrites from the Mount Princeton magmatic center[J]. Contributions to Mineralogy and Petrology, 165: 961～980.

Murphy M, Sparks R, Barclay J, *et al*. 2000. Remobilization of andesite magma by intrusion of mafic magma at the Soufriere Hills Volcano, Montserrat, West Indies[J]. Journal of Petrology, 41: 21～42.

Pallister J S, Hoblitt R P and Reyes A G. 1992. A basalt trigger for the 1991 eruptions of Pinatubo volcano? [J]. Nature, 356: 426～428.

Parmigiani A, Huber C and Bachmann O. 2014. Mush microphysics and the reactivation of crystal-rich magma reservoirs[J]. Journal of Geophysical Research: Solid Earth, 119: 6 308～6 322.

Perugini D, Valentini L and Poli G. 2007. Insights into magma chamber processes from the analysis of size distribution of enclaves in lava flows: A case study from Vulcano Island (Southern Italy)[J]. Journal of Volcanology and Geothermal Research, 166: 193～203.

Pietranik A, Slodczyk E, Hawkesworth C J, *et al*. 2013. Heterogeneous zircon cargo in voluminous late paleozoic rhyolites: Hf, O isotope and Zr/Hf records of plutonic to volcanic magma evolution[J]. Journal of Petrology, 54: 1 483～1 501.

Pistone M, Blundy J and Brooker R A. 2017. Water transfer during magma mixing events: Insights into crystal mush rejuvenation and melt extraction processes[J]. American Mineralogist, 102: 766～776.

Pritchard M E, Silva S L D, Michelfelder G. *et al*. 2018. Synthesis: PLUTONS: Investigating the relationship between pluton growth and volcanism in the Central Andes[J]. Geosphere, 14: 954~982.

Przybyło A, Pietranik A and Schulz B. 2020. Towards identification of zircon populations in Permo-Carboniferous rhyolites of Central Europe: Insight from automated SEM-mineral liberation analyses [J]. Minerals, 10(4): 308.

Reid M R, Vazquez J A and Schmitt A K. 2011. Zircon-scale insights into the history of a Supervolcano, Bishop Tuff, Long Valley, California, with implications for the Ti-in-zircon geothermometer[J]. Contributions to Mineralogy and Petrology, 161(2): 293~311.

Reubi O and Blundy J. 2009. A dearth of intermediate melts at subduction zone volcanoes and the petrogenesis of arc andesites[J]. Nature, 461: 1 269~1 273.

Rooney T O and Deering C D. 2014. Conditions of melt generation beneath the Taupo Volcanic Zone: The influence of heterogeneous mantle inputs on large-volume silicic systems[J]. Geology, 42(1): 3~6.

Ruprecht P and Bachmann O. 2010. Pre-eruptive reheating during magma mixing at Quizapu volcano and the implications for the explosiveness of silicic arc volcanoes[J]. Geology, 38(10): 919~922.

Samperton K M, Schoene B, Cottle J M, *et al*. 2015. Magma emplacement, differentiation and cooling in the middle crust: Integrated zircon geochronological-geochemical constraints from the Bergell Intrusion, Central Alps[J]. Chemical Geology, 417: 322~340.

Sano Y, Terada K and Fukuoka T. 2002. High mass resolution ion microprobe analysis of rare earth elements in silicate glass, apatite and zircon: Lack of matrix dependency[J]. Chemical Geology, 184: 217~230.

Scaillet B, Holtz F and Pichavant M. 1998. Phase equilibrium constraints on the viscosity of silicic magmas: 1. Volcanic-plutonic comparison [J]. Journal of Geophysical Research: Solid Earth, 103(B11): 27 257~27 266.

Scandone R, Cashman K V and Malone S D. 2007. Magma supply, magma ascent and the style of volcanic eruptions[J]. Earth and Planetary Science Letters, 253: 513~529.

Schoene B, Latkoczy C, Schaltegger U, *et al*. 2010. A new method integrating high-precision U-Pb geochronology with zircon trace element analysis (U-Pb TIMS-TEA)[J]. Geochimica et Cosmochimica Acta, 74: 7 144~7 159.

Siégel C, Bryan S E, Allen C M, *et al*. 2018. Use and abuse of zircon-based thermometers: A critical review and a recommended approach to identify antecrystic zircons[J]. Earth-Science Reviews, 176: 87~116.

Sillitoe R H. 2010. Porphyry copper systems[J]. Economic Geology, 105(1): 3~41.

Sliwinski J T, Bachmann O, Ellis B S, *et al*. 2015. Eruption of shallow crystal cumulates during explosive phonolitic eruptions on Tenerife, Canary Islands[J]. Journal of Petrology, 56(11): 2 173~2 194.

Słodczyk E and Breitkreuz C. 2014. Zircon abundance, size and paragenesis in SiO_2-rich volcanic rocks: Implications for geochronologic studies[J]. Geoscience Notes, 2: 15~35.

Stelten M E, Cooper K M, Vazquez J A, *et al*. 2015. Mechanisms and timescales of generating eruptible rhyolitic magmas at Yellowstone caldera from zircon and sanidine geochronology and geochemistry [J]. Journal of Petrology, 56(8): 1 607~1 642.

Storm S, Shane P, Schmitt A K, *et al*. 2011. Contrasting punctuated zircon growth in two syn-erupted rhyolite magmas from Tarawera volcano: Insights to crystal diversity in magmatic systems[J]. Earth and Planetary Science Letters, 301: 511~520.

Szymanowski D, Fehr M A, Guillong M, *et al*. 2018. Isotope-dilution anchoring of zircon reference materials for accurate Ti-in-zircon thermometry[J]. Chemical Geology, 481: 146~154.

Szymanowski D, Wotzlaw J F, Ellis B S, *et al*. 2017. Protracted near-solidus storage and pre-eruptive rejuvenation of large magma reservoirs[J]. Nature Geoscience, 10: 777~782.

Tapster S, Condon D, Naden J, *et al*. 2016. Rapid thermal rejuvenation of high-crystallinity magma linked to porphyry copper deposit formation: Evidence from the Koloula Porphyry Prospect, Solomon Islands [J]. Earth and Planetary Science Letters, 442: 206~217.

Tibaldi A. 2015. Structure of volcano plumbing systems: A review of multi-parametric effects[J]. Journal of Volcanology and Geothermal Research, 298: 85~135.

Trail D, Watson E B and Tailby N D. 2012. Ce and Eu anomalies in zircon as proxies for the oxidation state of magmas[J]. Geochimica et Cosmochimica Acta, 97: 70~87.

Ustiyev Y K. 1965. Problems of volcanism and plutonism. Volcano-plutonic formations[J]. International Geology Review, 7: 1 994~2 016.

Walker B A, Klemetti E, Grunder A, *et al*. 2013. Crystal reaming during the assembly, maturation, and waning of an eleven-millionyear crustal magma cycle: Thermobarometry of the Aucanquilcha volcanic cluster[J]. Contributions to Mineralogy and Petrology, 165: 663~682.

Watson E B. 1996. Surface enrichment and trace-element uptake during crystal growth[J]. Geochimica et Cosmochimica Acta, 60: 5 013~

5 020.

Watson E B and Liang Y. 1995. A simple model for sector zoning in slowly grown crystals: Implications for growth rate and lattice diffusion, with emphasis on accessory minerals in crustal rocks[J]. American Mineralogist, 80(11~12): 1 179~1 187.

Watson E B, Wark D A and Thomas J B. 2006. Crystallization thermometers for zircon and rutile[J]. Contributions to Mineralogy and Petrology, 151: 413~433.

Watts K E, Bindeman I N and Schmitt A K. 2012. Crystal scale anatomy of a dying supervolcano: An isotope and geochronology study of individual phenocrysts from voluminous rhyolites of the Yellowstone caldera [J]. Contributions to Mineralogy and Petrology, 164(1): 45~67.

Weinberg R F. 2006. Melt segregation structures in granitic plutons[J]. Geology, 34(4): 305~308.

Wotzlaw J F, Schaltegger U, Frick D A, *et al*. 2013. Tracking the evolution of large-volume silicic magma reservoirs from assembly to supereruption[J]. Geology, 41(8): 867~870.

Wu Fuyuan, Liu Xiaochi, Ji Weiqiang, *et al*. 2017. Highly fractionated granites: Recognition and research[J]. Science China Earth Sciences, 60: 1 201~1 219.

Xu X, Zhao K, He Z, *et al*. 2020. Cretaceous volcanic-plutonic magmatism in SE China and a genetic model[J/OL]. Lithos, https://doi.org/10.1016/j.lithos.2020.105 728.

Yan L, He Z, Beier C, *et al*. 2018a. Geochemical constraints on the link between volcanism and plutonism at the Yunshan caldera complex, SE China[J]. Contributions to Mineralogy and Petrology, 173: 4.

Yan L L, He Z Y, Beier C, *et al*. 2018b. Zircon trace element constrains on the link between volcanism and plutonism in SE China[J]. Lithos, 320~321: 28~34.

Yan L L, He Z Y, Jahn B M, *et al*. 2016. Formation of the Yandangshan volcanic-plutonic complex (SE China) by melt extraction and crystal accumulation[J]. Lithos, 266~267: 287~308.

Yan L L, He Z Y, Klemd R, *et al*. 2020. Tracking crystal-melt segregation and magma recharge using zircon trace element data[J]. Chemical Geology, 542: 119 596.

Zhang C C, Sun W D, Wang J T, *et al*. 2017. Oxygen fugacity and porphyry mineralization: A zircon perspective of Dexing porphyry Cu deposit, China[J]. Geochimica et Cosmochimica Acta, 206: 343~363.

Zhang J H, Yang J H, Chen J Y, *et al*. 2018. Genesis of late Early Cretaceous high-silica rhyolites in eastern Zhejiang Province, southeast China: A crystal mush origin with mantle input[J]. Lithos, 296~299: 482~495.

Zimmerer M J and Mcintosh W C. 2012. An investigation of caldera-forming magma chambers using the timing of ignimbrite eruptions and pluton emplacement at the Mt. Aetna caldera complex[J]. Journal of Volcanology and Geothermal Research, 245: 128~148.

Zou X, Qin K, Han X, *et al*. 2019. Insight into zircon REE oxy-barometers: A lattice strain model perspective[J]. Earth and Planetary Science Letters, 506: 87~96.

附中文参考文献

罗照华, 杨宗锋, 代　耕, 等. 2013. 火成岩的晶体群与成因矿物学展望[J]. 中国地质, 40(1): 176~181.

马昌前, 邹博文, 高　珂, 等. 2020. 晶粥储存、侵入体累积组装与花岗岩成因[J]. 地球科学, 45(12): 4 332~4 351.

吴福元, 刘小驰, 纪伟强, 等. 2017. 高分异花岗岩的识别与研究[J]. 中国科学: 地球科学, 47(7): 745~765.